e-Polymers **2011**, no. 071

http://www.e-polymers.org

ISSN 1618-7229

SPPO/PEI-based acid-base blend membranes for direct methanol fuel cells

Wen-Chin Tsen,[1] Fu-Sheng Chuang,[1] Yao-Chi Shu,[1] Chien-Chung Chen,[2] Chunli Gong,[3] Sheng Wen[3]*

[1*]Department of Polymer Materials, Vanung University, Tao-Yuan, Taiwan 32045, Republic of China, fax 886 3 4333063 ; e-mail: ycs1226@mail.vnu.edu.tw.
[2]Graduate Institute of Biomedical Materials and Engineering, Taipei Medical University, Taipei Taiwan 110, Republic of China.
[3]Department of Chemistry, Xiaogan University, Xiaogan, Hubei 432100, China.

(Received: 27 April, 2009; published: 30 July, 2011)

Abstract: New acid-base polymer blends based on sulfonated poly(phenylene oxide) (SPPO) as the proton-conducting component and poly(ether imide) (PEI) as the basic component were considered for use as proton-exchange membranes (PEM). The obtained blend membranes had a higher thermal stability and a higher glass transition temperature (T_g) than the pure SPPO, as revealed by TGA and DSC. The morphology of blend membranes indicated that PEI was highly compatible with SPPO polymers because of the formation of hydrogen bonds between the sulfonated acid and PEI. Although the blend membranes exhibited a lower water uptake and lower proton conductivity than the pure SPPO membrane, the PEI component improved the dimensional stability, mechanic properties, and especially inhibited methanol permeation. The methanol permeability coefficient of the blend membrane with 30 wt.% PEI content was 9.68×10^{-8} cm^2/s, which is lower than that of the pure SPPO and just one tenth of that of Nafion® 112. This considerable reduction in methanol crossover revealed the feasibility of the blend membranes as promising electrolytes for direct methanol fuel cells.
Keywords: Sulfonated poly(phenylene oxide); Poly(ether imide); Polymer blend; Proton exchange membrane; Fuel cells.

Introduction

Fuel cells have been identified as a very feasible energy source with minimal noxious emissions and have been the subject of academic and industrial interest for over a decade [1]. Among the various fuel cells, direct methanol fuel cells (DMFCs) are the most suitable for vehicles (cars, trucks, and buses) or portable devices (cell phones and laptops) because they have a high charge density, low operating temperature, and simple fuel-cell setup (with easy storage of methanol and no need for a reformer) [2-5]. The electrolyte is the most important component in any fuel-cell system. One of the main components in DMFCs is the proton exchange membrane (PEM). Dupont Nafion® or other perfluorinated sulfonic acid membranes are widely acknowledged to be electrolyte membranes because of their high proton conductivity and chemical stability. However, Nafion® membranes have some drawbacks [6, 7]: (i) Nafion® is too expensive and difficult to process; (ii) there is a strong dependence on relative humidity in maintaining the proton conductivity of Nafion® membranes. This is the reason why proton conductivity decreases with the dehydration at high temperature; (iii) thermal instability at high temperature. This property causes the membrane to

physically shrink during high temperature operation, with subsequent poor contact and proton conductivity between the membrane and the electrodes; (iv) high methanol permeability, which not only wastes fuel but also reduces cell performance for application in DMFCs.

Contemporary electrolyte membrane research involves the development of new polymer electrolytes that are based on hydrocarbon polymers [8]. The main approach, which is presently of considerable interest to industry and has been adopted by numerous researchers, involves the attachment of sulfonic acid groups onto various low-cost aromatic polymers with high thermal, chemical and oxidative stability and good mechanical properties. Examples include sulfonated poly(arylene ether sulfone) [9-11], sulfonated poly(ether ether ketone) [12-15], sulfonated polyimides [16-19] and others. However, when their ion-exchange capacities (IEC) values are comparable, the stronger acidity of the perfluorosulfonic acid than of sulfonated hydrocarbon polymers results in higher proton conductivities [20]. Therefore, the sulfonated hydrocarbon polymer with a high IEC value was prepared to achieve sufficient proton conductivity. Yet, the increase in the concentration of sulfonated groups in the membranes is responsible for poor mechanical properties when they are very swollen by water.

Acid-base blend membranes, wherein a sulfonated polymer with high proton conductivity is combined with a basic polymer component, are employed because they retain mechanical integrity. They have become popular for use in newly designed improved PEM materials [21-24]. Various acid–base blend membranes ionically crosslinked polymer membranes from sulfonated poly(aryl ether ether ketone) [21,23] and sulfonated polysulfone [25,26] as acidic polymers and polybenzimidazole [24], basic polysulfone [25] and other commercial polymers such as poly(amide imide) [21,27] as basic polymers. These blend membranes perform well in direct methanol fuel cells [21]. Covalently and ionically crosslinked membranes have homogeneous membrane morphology. This approach leads the way to new combinations of acidic and basic polymers to make new families of electrolyte membranes for DMFCs applications.

In this study, a new system of an ionomer with high IEC (SPPO 2.63) in combination with PEI as the basic component was adopted for evaluation as a composite PEM. The morphologies and properties, including thermal, water uptake, mechanical properties and proton conductivities, are varied by varying the composition of the blend.

Results & Discussion

Determination the IEC of SPPO

Fig.1 presents the ^{1}H-NMR spectra of PPO and SPPO. As for the PPO, the low field 6.4 ppm is the peak of the aromatic protons, and the upfield signals (2.08–2.18 ppm) are associated with the 6H of the methyl groups on the aromatic ring. After sulfonation, the sulfonic group in the repeat unit results in a shift of the signal from protons attached to the methyl group in the ortho position to the sulfonic group, and that from the aromatic proton of the substituted unit. As shown in Fig. 1(b), the two peaks of low field 6.52 and 6.35 ppm belong to the proton of the sulfonated and unsulfonated aromatic proton, respectively. The upfield peak 2.49 ppm is due to the protons of the methyl group in the ortho-position to the sulfonic group, and the

signals (2.01–2.08 ppm) belong to the $–CH_3$ in the para-position to the $–SO_3H$. It can be observed that the chemical shift of the aromatic proton moves to the low field because of the strong induction of $–SO_3H$. Therefore, the NMR spectrum of SPPO shows two extra signals in addition to those of PPO. The degree of sulfonation can be calculated considering the intensities of the additional signals. Derived from the Eq. (1), a calculated DS of 40.1% was measured by NMR technique, that is, the ion exchange capacity (IEC) was 2.63 meq/g.

$$\frac{I_{a'}}{I_a} = \frac{DS}{2-2DS} \tag{1}$$

where, $I_{a'}$ is the intensity of $H_{a'}$ and the I_a is the intensity of the unsulfonated aromatic protons.

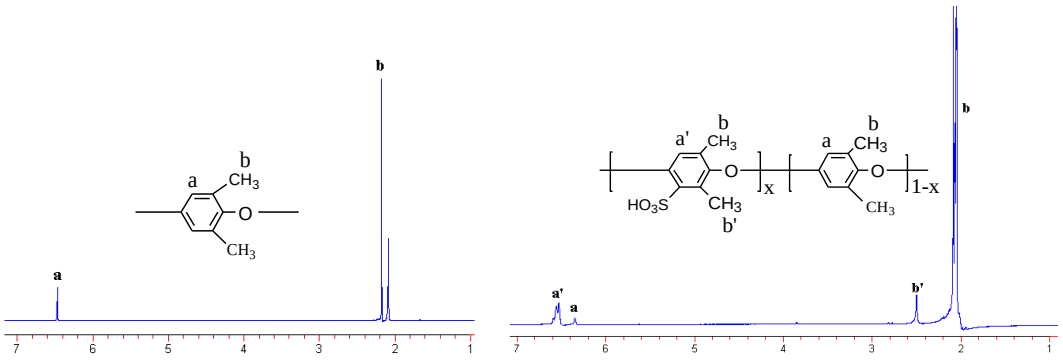

Fig. 1. ^{1}H-NMR spectra of (a) PPO and (b) SPPO.

FTIR

FTIR spectra were obtained to confirm the incorporation of PEI into the blend membranes.

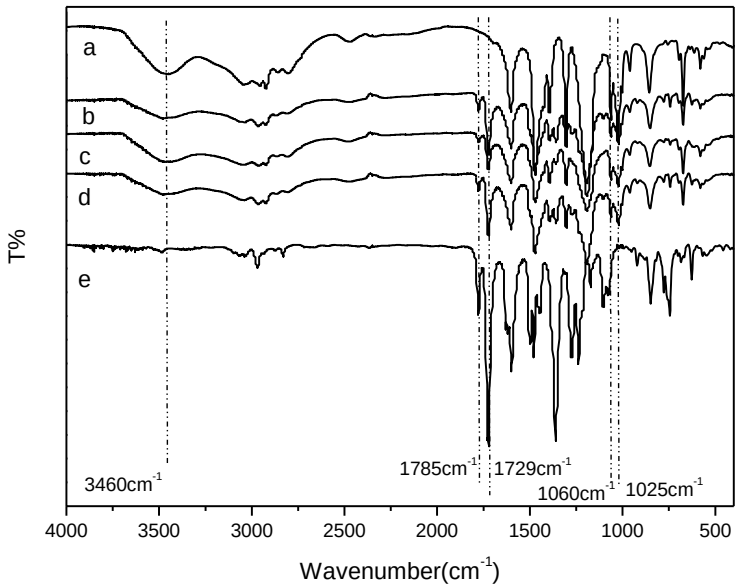

Fig. 2. FTIR spectra of (a)SPPO, (b)SPPO/PEI 80/20, (c) 70/30, (d) 50/50, (e) PEI.

Fig. 2 shows the FTIR spectra of the SPPO, SPPO/PEI 80/20, SPPO/PEI 70/30, SPPO/PEI 50/50 and PEI membranes. The symmetric and asymmetric stretches of the sulfonated groups of the blend membranes appeared at 1060 cm^{-1} and 1025 cm^{-1}, respectively. The broad absorption band at 3600 cm^{-1} was assigned to the O-H vibration associated with the interaction between the sulfonic acid groups and molecular water. The peaks at 1362 cm^{-1}, 1237 cm^{-1} and 1275 cm^{-1} are attributable to the aromatic ether vC-O-C. The stretching vibrations of the aromatic ring bone were in the 1446 cm^{-1}~1630 cm^{-1} wave band. The double peaks at 1729 cm^{-1} and 1785 cm^{-1} are the characteristic absorption bands of vC=O in the imide ring. The intensities of these two characteristic peaks increased with the PEI content in the blend membranes. These spectral data confirmed the successful incorporation of PEI in the blend membranes.

Thermal stability of membranes

The thermal stability of the blend membranes was studied using TGA. Fig. 3 indicates that the TGA curves of the SPPO/PEI blend membranes in an atmosphere of nitrogen are very similar to that of the pure SPPO membrane. Each TGA curve includes two distinct weight loss steps, of which the first, at about 240 ^{0}C, was associated mainly with the splitting of aromatic sulfonic acid groups of SPPO. The second weight loss region at about 410 ^{0}C was attributed to the decomposition of the main chain of the polymers. Fig. 3 also reveals that the blend membranes are a little more thermally stable than the pure SPPO membranes, so a hypothesis has been established that the incorporation of PEI into the highly charged SPPO limits the mobility of the SPPO hydrophilic cluster by the intermolecular interaction between SPPO and PEI. Meanwhile, the fact that stability of the PEI backbone (whose temperature of initial decomposition is about 500 ^{0}C [31]) exceeds that of the PPO main chain (whose temperature of initial decomposition is ca. 450 ^{0}C [29]) may explain the higher thermal stability.

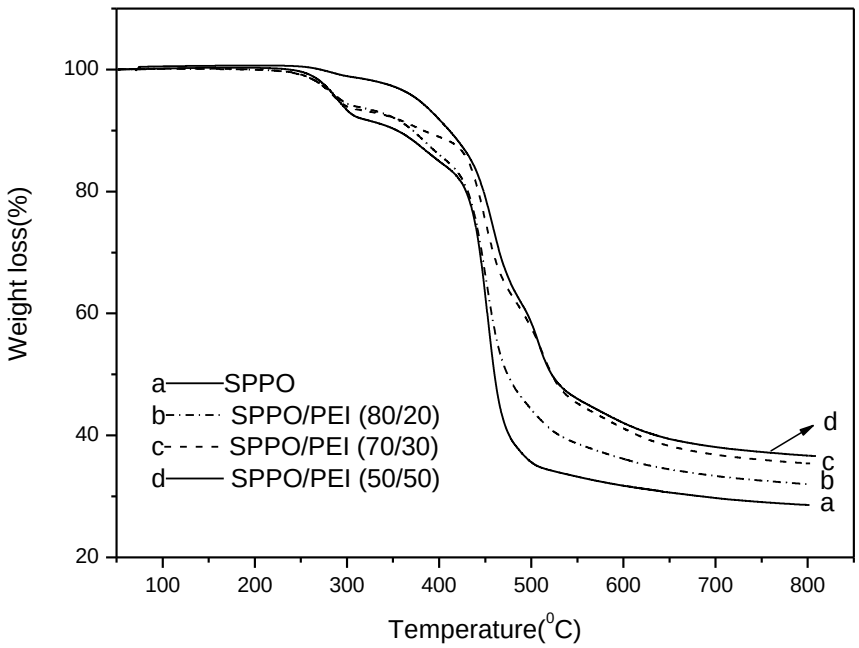

Fig. 3. The thermogravimetric curves for SPPO and blend membranes.

Blend morphology

As reported in the literature [32], the electrochemical properties of proton exchange membranes are closely associated with their morphology. Scanning electron microscopy (SEM) was performed to examine the morphology of the blend membranes. As shown in Fig.4 and Fig.5, the SPPO membrane has a homogeneous morphology. A very fine island-like, somewhat larger microstructure was observed in the SPPO/PEI 80/20 blend. The large microphase-separation between the acidic and the basic blend component appeared at in this composition because the interaction forces are not strong enough to lead to complete miscibility. As the PEI content in the blends increased, the microphase decreased. The micrograph of the SPPO/PEI 50/50 blend clearly shows that the polymers exhibit very fine microstructures with uniform and more compact morphology and without evident phase separation.

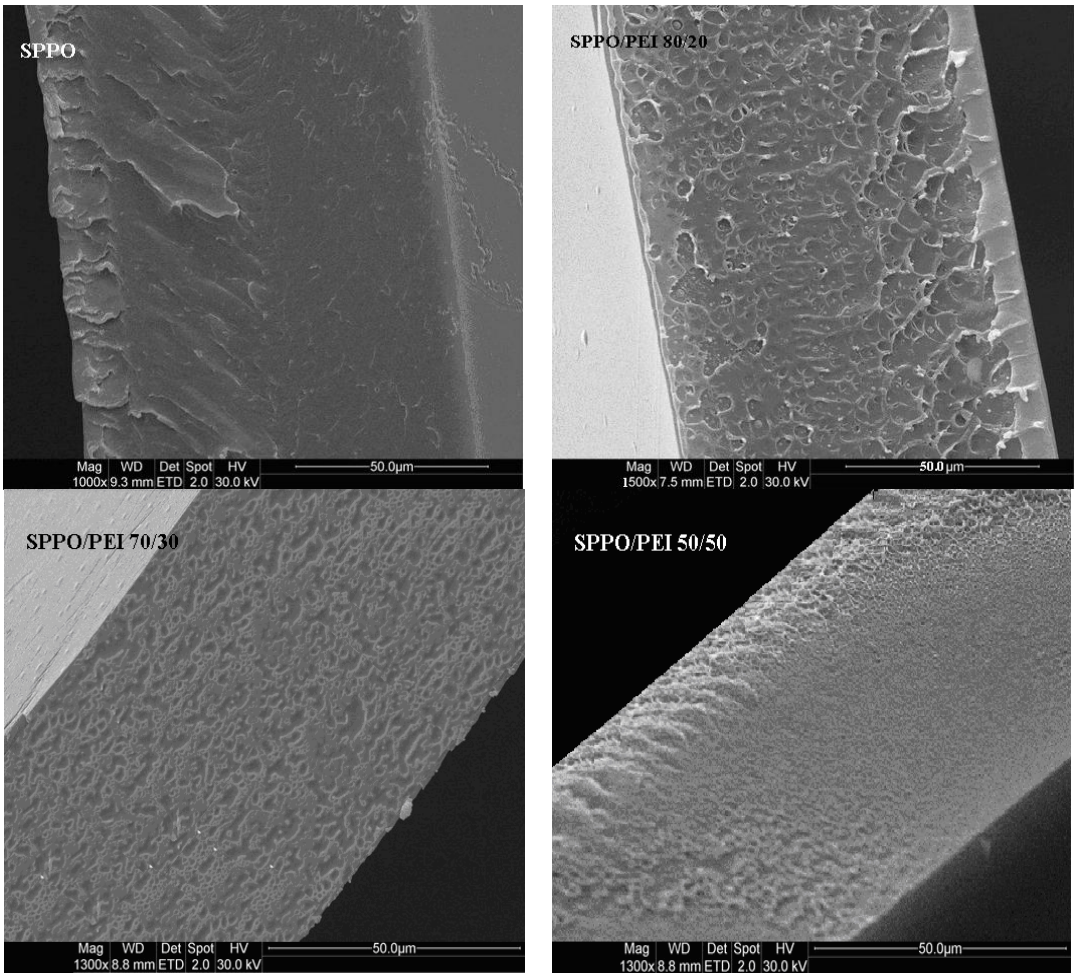

Fig. 4. Cross-sectional SEM micrographs of the SPPO/PEI blend membranes at low magnification.

Another indication of a phase-separated morphology in a polymer blend is two glass transitions [27]. However, since the T_g values of SPPO and PEI are close to each other (T_g ($SPPO_{2.63}$)=230 ^{0}C, T_g(PEI)=220 ^{0}C), DSC was unable to distinguish between two co-existing phases in the membranes. As presented in Fig. 6, only a single, though broad, composition-dependent T_g was detected. Furthermore, the blending of sulfonated polymer with basic polymer has a strong impact on T_g.

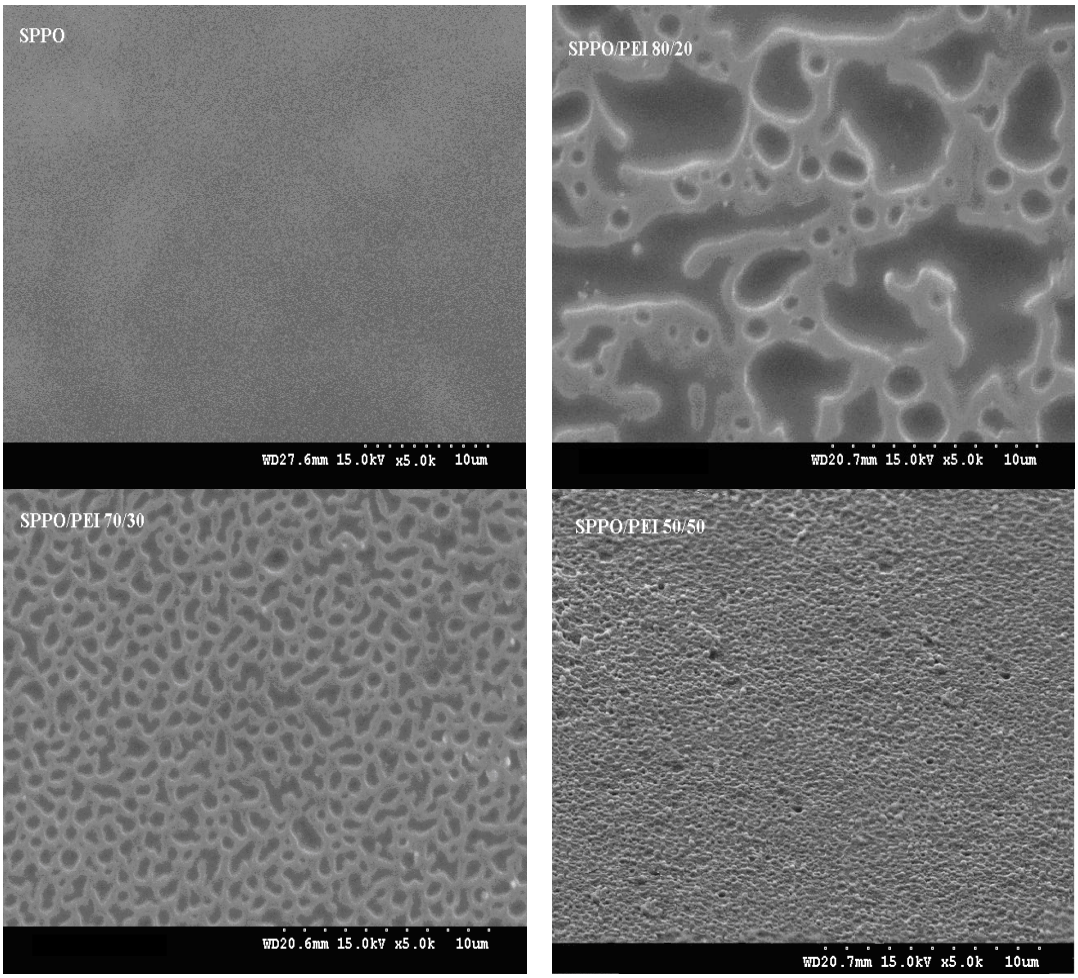

Fig. 5. Cross-sectional SEM micrographs of the SPPO/PEI blend membranes at high magnification.

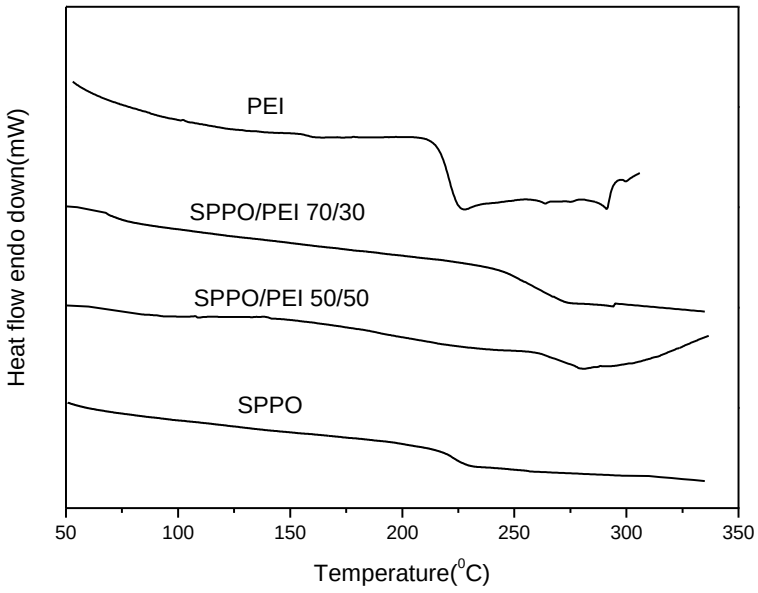

Fig. 6. DSC thermograms of PEI and the blends.

For example, the T_g of the SPPO sample is 230 ^{0}C; that of PEI is 220 ^{0}C, and that of the SPPO/PEI 70/30 blend is 255 ^{0}C. The large increase in T_g by 25 ^{0}C from SPPO to the SPPO/PEI 70/30 blend is caused by the acid-base interactions between the acidic and basic components of the blend. Similar findings have been observed for other acid-base polymer blend systems, such as SPEEK/PSU$(NH_2)_2$ blends [24] and SPSU/P4VP blends [25].

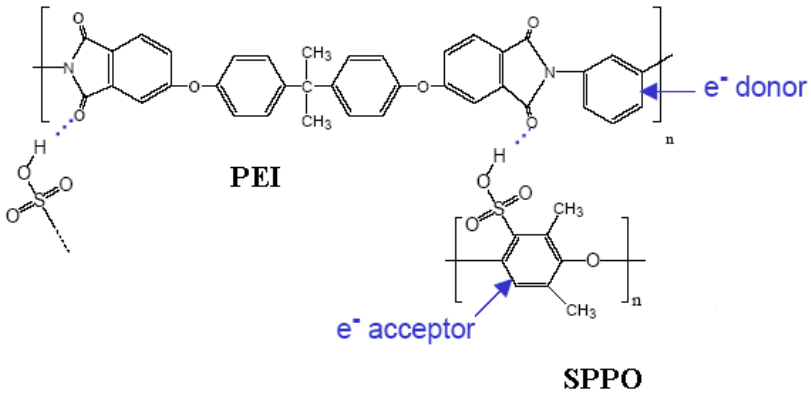

Scheme 1. The formation of hydrogen bond between SPPO and PEI.

Water uptake

The ability to take up water is an important property of sulfonated polymer that enables it to be used in fuel cells. The proton conductivity of the polymer generally increases with water uptake: the uptake of more water improves the formation of the hydrophilic domain which conducts protons [12]. The water uptake of the polymer can be increased by increasing the ionic group content in the polymer chain, but most often, the uptake of more water increases the swelling of a membrane, reducing its mechanical stability and leading to a high methanol permeability. Accordingly, water uptake and polymer swelling must be optimized for successful operation in fuel cells.

Table 1 presents the percentage of the saturated (48 h equilibration) sorption of water in pure SPPO and SPPO/PEI blend membranes at room temperature and 80 ^{0}C. As expected, the water uptake decreased as the weight fraction of PEI in the blends increased. For example, the water uptake of pure SPPO membrane is nearly 26.8% at room temperature, whereas, SPPO/PEI blend membranes have a water uptake of 21.6%, 18.76%, 13.09%, 9.87% and 6.57%, with the weight ratios of SPPO to PEI from 90/10 to 50/50 in equal increments. The water uptake decreases as PEI is added to SPPO, accounting for the hydrophobicity of PEI and the formation of hydrogen bonding between PEI and sulfonic acid groups (Scheme 1). However, the amount of hydrogen bonds generated between PEI and sulfonic acid groups increases with the PEI content, reducing the excessive swelling of the polymer under wet conditions and thereby improving the mechanical properties of the blend membranes. This conclusion was confirmed by the dimensional change data, which is listed in Table 1. SPPO/PEI blends with PEI contents from 20 to 30% exhibited the optimum water uptake and dimensional stability.

Tab. 1. The water uptake and dimensional change of the blend membranes.

Samples	Water uptake (%)		Dimensional change (%)		
	20℃	80℃	Length	Width	Thickness
SPPO	24.80	35.58	35.9	17.3	56.2
SPPO/PEI 90/10	21.60	31.30	29.5	11.2	48.9
SPPO/PEI 80/20	18.76	26.75	17.4	10.5	27.1
SPPO/PEI 70/30	13.09	20.62	14.6	9.7	22.4
SPPO/PEI 60/40	9.87	13.69	11.9	10.1	16.6
SPPO/PEI 50/50	6.57	10.79	9.4	6.8	14.6
Nafion® 112	15.04	26.08	15.0	4.7	28.0

Tensile properties

The mechanical properties of a membrane affect the manufacturing conditions of the membrane electrode assembly (MEA) and the durability of the DMFCs, since the temperature, pressure and humidification vary frequently during DMFCs operation. Here, membranes underwent tensile testing at room temperature and 80 ℃, yielding the results in Table 2. For comparison, the Nafion® 112 membrane was also tested under the same set of conditions. The Nafion® 112 membrane had a Young's modulus of 240.5 MPa, elongation at breaking of 310 %, and a maximum stress of 27.10 MPa at breaking, these values are quite consistent with the Nafion® product information provided by DuPont [34] under similar ambient conditions.

Tab. 2. The mechanical properties of the blend membranes.

Samples	Young's modulus (MPa)		Tensile strength (MPa)		Elongation (%)		Methanol permeability (cm^2/s)
	20 ^{0}C	80 ^{0}C	20^{0}C	80 ^{0}C	20^{0}C	80^{0}C	
SPPO	1030.2	896.3	33.10	27.64	21.50	30.58	8.62×10^{-7}
SPPO/PEI 90/10	1096.4	890.6	37.55	31.71	18.24	31.30	5.08×10^{-7}
SPPO/PEI 80/20	1126.3	930.4	40.50	34.94	15.88	26.74	2.03×10^{-7}
SPPO/PEI 70/30	1247.3	1080.2	47.30	40.46	12.09	20.62	9.68×10^{-8}
SPPO/PEI 60/40	1357.5	1217.7	50.72	45.11	14.87	25.69	6.78×10^{-8}
SPPO/PEI 50/50	1558.4	1387.6	58.94	52.16	19.57	28.79	3.23×10^{-8}
Nafion® 112	240.5	106.7	27.10	12.11	310	408	1.05×10^{-6}

The initial Young's moduli of the membranes of SPPO, SPPO/PEI 90/10, 80/20, 70/30, 60/40 and 50/50 were 1.03 GPa, 1.09 GPa, 1.13 MPa, 1.25 GPa, 1.36GPa and 1.56 GPa, respectively, which varies greatly from that of the Nafion® 112 membrane. Meanwhile, Table 1 reveals that the amount of PEI in the sulfonated polymers significantly affects their mechanical properties. The modulus and tensile strength of the membranes at room temperature increased with the PEI content. The high strength and stiffness of the composite membranes were attributed to the rigidity of PEI and the hydrogen bond between the sulfonic acid groups and the basic polymer. The elongation at breaking of the blend membranes declined as the basic polymer content increased to 40 %, and then increased as the PEI content was increased further. This fact may be explained as follows; ionic cross-linking between the acidic polymer and basic polymer when the PEI content is below 40% reduces the mobility of the chains, reducing the elongation at breaking. However, as the PEI

content increased above 40 %, the flexibility of PEI increased clearly because of the formation of PEI continuous phase in the blends.

Since PEMs in fuel cells are generally operated at temperatures close to 80 ^{0}C, the mechanical properties of these membranes were measured. Table 2 presents the results. The Young's modulus and tensile strength of the blend membranes decreased somewhat. However, the elongation at break increased significantly because the high temperature increased the flexibility of the chain. These data indicate that these blend membranes are strong and tough both at room and high temperature and are very promising for use in DMFCs.

Proton Conductivity

The proton conductivity is a decisive property of fuel cell membranes as the efficiency of the fuel cell depends on the proton conductivity. Proton conductivity directly depends on the uptake of water and the IEC of the sulfonated polymer. The conductivity data of the pure SPPO and blend membranes were measured in the longitudinal direction by AC impedance spectroscopy as the temperature increased, and are plotted in Fig. 7. The conductivity values of the prepared membranes were compared to those of commercial Nafion® 112 to ascertain its usefulness.

The pure SPPO membrane exhibits lower proton conductivity than Nafion® 112 at room temperature and up to 80 ^{0}C, because of the flexible main chain of Nafion®, which leads to extensive swelling of the membrane in the hydrated state and easy percolation of protons. Moreover, the unique hydrophilic-hydrophobic phase segregated structure causes Nafion® to form clusters with ion-rich channels, accounting for the high proton conduction at low temperature [33].

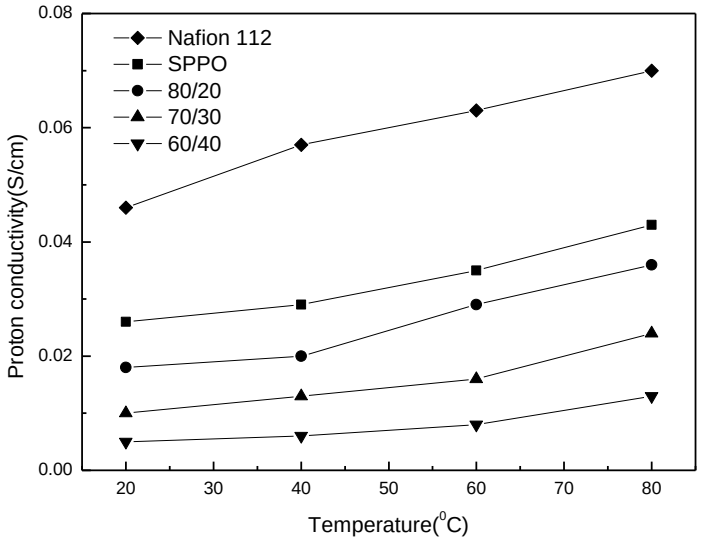

Fig. 7. Proton conductivities of the membranes at different temperatures.

Methanol permeability

Membranes for the practical usage in DMFCs must both possess high proton conductivity and low methanol permeability [21]. The high methanol crossover for Nafion® membrane in the DMFCs application is one of the most significant drawbacks that make them impractical for large-scale production. The methanol

permeability of the blend membranes is shown in Table 2. The methanol permeability of the blend membranes decreased obviously compared to the pure SPPO membrane. With the increase of the content of PEI, the methanol permeability of the blend membranes decreased. Assuming that the methanol mostly passes through a channel where ion cluster forms, there is a reasonable explanation for methanol permeability of blend membranes. As discussed in morphology of blend membranes detected by SEM, it was shown that the membranes become more compact and the hydrophilic domain size becomes smaller than the SPPO membranes because of the formation of hydrogen bond of the blend membranes. So this will lead to the decreasing of proton conductivity and methanol permeability with the PEI content increasing.

The selectivity (S), the ratio of proton conductivity and methanol permeability, is often applied to evaluate the potential performance of DMFCs [34]. The S values of membranes investigated in this work are compared in Fig. 8. When the PEI content is below 30 wt% in the blend membranes, the selectivity increased with increasing PEI content. The SPPO/PEI 30% membrane has the highest selectivity in our experiments, 1.03×10^{5} $S\cdot s\cdot cm^{-3}$, which is almost 3 times than that of Nafion® 112 membrane. This excellent selectivity of SPPO/PEI blend membranes could indicate a potential feasibility as a promising electrolyte for DMFCs.

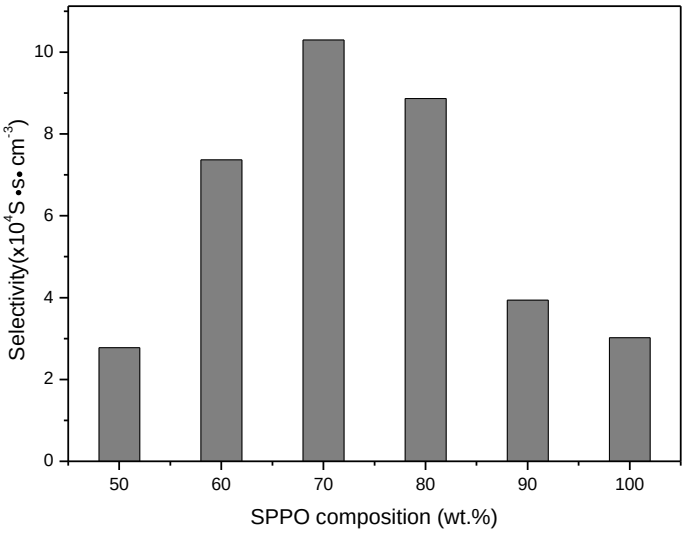

Fig. 8. The selectivity of SPPO/PEI blend membranes at different SPPO content.

Conclusions

A new system of SPPO/PEI acid-base blend membranes with various weight ratios was prepared. The effect of PEI on the properties of the blend membranes was evaluated in terms of thermal and dimensional stability, water uptake, morphology, tensile properties and proton conductivity. The blend membranes had higher T_g and thermal stability than the pure SPPO membranes. The dimensional stability notably increased with PEI content, because of an increase in hydrogen bond interactions, which prevent the excessive swelling of the membrane in water and thereby increase its mechanical stability. Methanol permeability was suppressed in the blend membranes with proper PEI content (about 20-30 wt.%). The excellent comprehensive property, especially the selectivity (the ratio of proton conductivity

and methanol permeability), of the blend membrane with 30 wt.% PEI content suggests its suitability as electrolyte in DMFC applications.

Experimental

Materials

PPO ([η]=0.4 dl/g in chloroform at 25 ^{0}C, General Electric Co.) was sulfonated in a chloroform solvent using chlorosulfonic acid as the sulfonating agent following the procedure described by us earlier [28, 29].The degree of sulfonation (DS) of the obtained SPPO was 40.1%, revealing that the ion exchange capacity (IEC) was 2.63 meq/g. PEI (Ultem1 1000) in pellet form was purchased from General Electric Corporation and dried for 8 h at 100 ^{0}C before use. Other chemicals were of analytical reagent grade and were used without further purification.

Preparation of blend membranes

Blends of calculated amounts of SPPO and PEI were dissolved in N,N-dimethylacetamide (DMAc) and oscillated homogeneously using an ultrasonic wave oscillator. Membranes with controlled thicknesses (dry membrane thickness 50～80μm) were prepared by casting the blend solutions onto clean glass plates and drying at 40 ^{0}C for 8 h, at 60 ^{0}C for 10 h, and then in a vacuum oven at 100 ^{0}C for 24 h. The membranes were carefully removed from the glass substrates using a sharp razor blade after they had been cooled to room temperature. Hereafter, the blend membranes are labeled SPPO/PES (a/b), where a/b is the ratio of the weights of SPPO and PEI.

^{1}H-NMR

The IEC value of SPPO was obtained by ^{1}H-NMR technique using a Varian Unity Inova 600 NMR spectrometer. Tetramethylsilane was used as the internal-standard chemical-shift reference. The ^{1}H-NMR spectrum of PPO was obtained at 20 ^{0}C in deuterated chloroform ($CDCl_3$). Deuterated acetone (CD_3COCD_3) was the selective solvent for dissolving SPPO.

FTIR

FTIR spectra were obtained using a Nicolet 380 Fourier transform spectrometer with a resolution of 2 cm^{-1}.

Thermogavimetric Analysis(TGA)

Thermogravimetric results were obtained with a thermogravimetry analyzer (SDT-Q600, TA Instruments New Castle, DE) at a heating rate of 10 ^{0}C /min in an N2 atmosphere.

Differential Scanning Calorimetry (DSC)

The glass transition temperatures were obtained using a Perkin-Elmer DSC-7 differential scanning calorimeter. Scans were conducted under nitrogen by heating to 220 ^{0}C, annealing at 220 ^{0}C for 10 min to eliminate thermal and solvent histories, and then quenching rapidly to room temperature. A DSC heating experiment was performed at 10 ^{0}C /min to measure T_g values as midpoints of the changes in the slope of the baseline.

Water Uptake

The blend membranes were dried in a vacuum oven at 100 ^{0}C for 24 h, and the dry weight (W_{dry}) was obtained. The samples were then immersed in deionized water at various temperatures for 48 h. Then, the wet membranes were blotted to remove surface water droplets and quickly weighed (W_{wet}). The water uptake of the membranes was calculated as follows.

$$\text{Water uptake (\%)} = \frac{W_{wet} - W_{dry}}{W_{dry}} \times 100\% \quad (2)$$

Tensile Test

The mechanical properties of the dumbbell specimens were measured using a high-temperature tension tester (GT-TFS2000, Gotech testing machines Inc., Taiwan) at a crosshead speed of 2 mm/min at 20 ^{0}C and 80 ^{0}C. The gauge length and width of the dumbbell specimens were 50 mm and 4 mm respectively. At least three specimens were tested for each sample and the results averaged.

Morphology

The cross-sectional morphology of the membranes was examined using a scanning electron microscope (SEM) X-650 from HITACHI. The membranes were fractured by brief immersion in liquid nitrogen. Fresh cross-sectional cryogenic fractures of the membranes were vacuum-sputtered with a thin layer of Pt/Pd prior to analysis.

Conductivity

The proton conductivities of blend membranes were measured using the AC impedance method. In a chamber, the tested membranes were placed into the clamp, connected by two platinum electrodes to a complex impedance analyzer (Solatron 1260 Impedance Analyzer) with a frequency range of 0.1Hz～10MHz and an AC voltage amplitude of 10mV. Before the proton conductivity was measured, all membranes were hydrated by immersion in deionized water for 24 h at room temperature. A sample of prehydrated membrane (3×3cm) was clamped between the two electrodes. The proton conductivity was calculated as follows [30].

$$\sigma = l / Rdw \quad (3)$$

where *l* is the distance between the electrodes; d and w are the thickness and width of the films, respectively, and R is the measured resistance.

Methanol Permeability

A two-compartment cell, as described in our previous work [31], was used to measure the methanol permeability of the membranes.

Initially one compartment *B* of the cell (V_B=20ml) was filled with 0.2 vol.% ethanol solution in deionized water. The other compartment A (V_A=20ml) was filled with 8 vol.% methanol and 0.2 vol.% ethanol and deionized water. The membrane with the diffusion area of 3.14 cm^2 sandwiched by O-ring shape Teflon was clamped between the two compartments. The membrane samples were equilibrated in deionized water for 24 h before testing. The diffusion cell was kept stirring slowly during experiment. The solution samples (about 2*μl*) in compartment *B* were taken at interval and were

detected by gas chromatography (GC-5890 series*II*, Hewlett Packard) using HP-20M (CARBOWAX 20M phase) chromatographic column together with a flame ionization detector (FID). Methanol permeability was calculated by following Eq.:

$$C_B = \frac{D \times K \times C_A \times A}{V_B \times L} \times t \quad (4)$$

where C_B is the methanol concentration in compartment *B*, C_A is the methanol concentration in compartment *A, A, L* and V_B are the diffusion area of membrane, the thickness and the solution volume of compartment *B. D, K* and *t* are the methanol diffusivity, the solubility and the permeability time, respectively. The methanol permeability, P_m, is defined as the product of diffusivity and solubility, *DK*.

References

[1] Lee, C.; Sundar, S.; Kwon, J.; Han, H. *J. Polym. Sci., Part A: Polym. Chem.* **2004**, 42, 3612.
[2] Li, X.; Chen, D.; Xua, D.; Zhao, C.; Wang, Z.; Lu, H.; Na, H. *J. Membr. Sci.* **2006**, 275,134.
[3] Li, X.; Liu, C.; Xua, D.; Zhao, C.; Wang, Z.; Zhang, G.; Na, H.; Xing, W. *J. Power Sources* **2006**, 162,1.
[4] Rhee, C. H.; Kim, H. K.; Chang, H.; Lee, J. S. *Chem. Mater.* **2005**, 17, 1691.
[5] Nagarale, R. K.; Gohil, G. S.; Shahi, V. K. *J. Membr. Sci.* **2006**, 280, 389.
[6] Tsai, J. C.; Kuo, J. F.; Chen, C. Y. *J. Power Sources* **2007**, 174, 103.
[7] Kim, H. J.; Krishnan, N. N.; Lee, S. Y. *J. Power Sources* **2006**, 160, 353.
[8] Rikukawa, M.; Sanui, K. *Prog. Polym. Sci.* **2000**, 25, 1463.
[9] Wang, F.; Hickner, Michael.; Kim,Y. S.; Zawodzinski, T. A.; McGrath, J. E. *J. Membr. Sci.* **2002**, 197, 231.
[10] Bai, Z.; Durstock, M. F.; Dang, T. D. *J. Membr. Sci.* **2006**, 281, 508.
[11] Kim, D. S.; Park, H. B.; Jang, J. Y.; Lee, Y. M. *J. Polym. Sci., Part A: Polym. Chem.* **2005**, 43, 5620.
[12] Xing,P.; Robertson, G. P.; Guiver, M. D.; Mikhailenko, S. D.; Kaliaguine, S. *Macromolecules* **2004**, 37, 7960.
[13] Mikhailenko, S. D.; Robertson, G. P.; Guiver, M. D.; Kaliaguine, S. *J. Membr. Sci.* **2006**, 285, 306.
[14] Zhong, S.; Liu, C.; Dou, Z.; Li, X.; Zhao, C.; Fu, T.; Na, H. *J. Membr. Sci*. **2006**, 285, 404.
[15] Kaliaguine, S.; Mikhailenko, S. D.; Wang, K. P.; Xing, P.; Robertson, G.; Guiver, M. *Catalysis Today* **2003**, 82, 213.
[16] Rahman, M. K.; Aiba, G.; Susan, M. A. B. H.; Sasaya, Y.; Ota, K.; Watanabe, M. *Macromolecules* **2004**, 37, 5572.
[17] Asano, N.; Aoki, M.; Suzuki, S.; Miyatake, K.; Uchida, H.; Watanabe, M. *J. Am. Chem. Soc.* **2006**,128, 1762.
[18] Fang, J.; Guo, X.; Harada, S.; Watari, T.; Tanaka, K.; Kita, H.; Okamoto, K. *Macromolecules* **2002,** 35,9022.
[19] Ye, X.; Bai, H.; Winston Ho, W. S. *J. Membr. Sci.* **2006**, 279, 570.
[20] Koter, S.; Piotrowski, P.; Kerres, J. *J. Membr. Sci.* **1999**,153, 83.
[21] Zhao, C.; Wang, Z.; Bi, D.; Lin, H.; Shao, K.; Fu,T.; Zhong, S.; Na, H. *Polymer* **2007**, 48, 3090.

[22] Jang, W.; Sundar, S.; Choi, S.; Shu, Y. G.; Han, H. *J. Membr. Sci.* **2006**, 280, 321.
[23] Fu, Y.; Manthiram, A.; Guiver, M. D. *Electrochem. Commun.* **2006**,1386.
[24] Kerres, J.; Ullrich, A.; Haring, T.; Preidel, W.; Baldauf, M.; Gebhardt, U. *J. New Mater. Electrochem. Syst.* **2000**, 3, 229.
[25] Kerres, J., Zhang, W.; Cui; W. *J. Polym. Sci.: Part A: Polym. Chem.* **1998**, 36, 1441.
[26] Kerres, J.; Ullrich, A.; Meier, F.; Haring, T. *Solid State Ionics* **1999**,125, 243.
[27] Swier, S.; Shaw, M.T.; Weiss, R. A. *J. Membr. Sci.* **2006**, 270, 22.
[28] Yang, S.; Gong, C.; Guan, R.; Zou, H.; Dai, H. *Polym. Adv. Technol.* **2006**, 17, 360.
[29] Guan, R.; Gong, C.; Lu, D.; Zou, H.; Lu, W. *J. Appl. Polym. Sci.* **2005**, 98, 1244.
[30] Damay, F.; Klein, L. C *Solid State Ionics* **2003**, 162–163, 261.
[31] Shu, Y. C.; Chuang, F. S.; Tsen, W. C.; Chow, J. D.; Gong, C.; Wen, S. *J. Appl. Polym. Sci.* **2008**,108,1783.
[32] Walker, M.; Baumgartner, K. M.; Kaiser, M.; Kerres, J.; Ullrich, A.; Rauchle, E. *J. Appl. Polym. Sci.* **1999**, 74, 67.
[33] Jang, W.; Choi, S.; Lee, S.; Shul, Y.; Han, H. *Polym. Degrad. Stab.* **2007**, 92, 1289.
[34] Shen,Y.; Qiu, X.; Shen, J.; Xi, J.; Zhu, W. *J. Power Sources* **2006**, 161, 54.